A New Robust Control to Improve the Dynamic Performance of Induction Motors

Guang Feng   Yan-Fei Liu
Department of Electrical and Computer Engineering,
Queens University, Kingston, Ontario, K7L 3N6
Email: guang.feng@ece.queensu.ca,
yanfei.liu@ece.queensu.ca

Lipei Huang
Department of Electrical Engineering, Tsinghua University,
Beijing, China, 100084
Email: huanglipei@mail.tsinghua.edu.cn

Abstract — **A nonlinear auto-disturbance rejection controller (ADRC) has been developed to ensure high dynamic performance in this paper. By using the extended state observer (ESO), ADRC can estimate accurately the derivative signals and accurate decoupling of induction motor is achieved too. In addition, the proposed strategy doesn't require knowledge of induction motor parameters. The simulation and experiment results show that the controller operates quite robustly under modeling uncertainty and external disturbance, and it is concluded that the proposed topology produces better dynamic performance such as small overshoot and fast transient time in the speed control than classical PID controller.**

I. INTRODUCTION

Research interest in high performance control of induction motors for all operation conditions has grown rapidly in the industry. At present, vector control has found widespread use because of its capability of torque/flux decoupling which gives high dynamic response and accurate motion control. However, in real-time implementation, precise decoupling which require accurate motor parameters can't be fully realized due to significant plant uncertainties such as external disturbances, unpredictable parameter variations and unmodeled plant nonlinear dynamics [1]. This may deteriorate the dynamic performance of flux and torque significantly. Generally speaking, the performance of this control system depends on the accurate mathematical model of induction motors [2]. Conventional approach in vector control is to use PID controllers to manipulate the static and dynamic performance of control system. In PID controller, the derivatives of the signals are required in order to achieve control objectives, such as reduced response time and reduced overshoot during transient conditions. Unfortunately, the derivatives of signals are difficult to retrieve because of noise. Furthermore, PID controller has many disadvantages: the transient performance of the loop is poor, and it is often dependent on the operating conditions. To overcome these problems, a great deal of research has been made into alternative control techniques. In recent years, adaptive methods and predict PID controllers appeal much more promising in the improvement of the robustness and dynamic performance of control systems [3-7]. However, they are very complicated and require some knowledge of model parameters and estimation of some model states. Therefore, they have much computational intensity in the real-time

implementation, and may lead to a very tedious job in the online debugging.

The main objective of this paper is to introduce a new configuration called Auto-Disturbance Rejection Controller (ADRC) developed for improving dynamic performance of induction motors. The core of ADRC is the extended state observer (ESO), which is based on the concept of generalized derivative. Using the extended state observer, ADRC can realize accurate decoupling of induction motor by monitoring state variables and their derivative signals accurately. In addition, the external disturbances and parameter variations could also be estimated and compensated by ADRC, so that the accurate model of induction model is not required. That means the design of ADRC is inherently independent of the controlled system model and its parameters, so this controller has the advantage of good adaptability and robustness. In simulation and experiments, this paper presents a detailed comparison of classic PID controller and ADRC under different operating conditions. Results show that ADRC can provide better dynamic performance under large variations of drive system parameters and load conditions.

II. CONTROL STRATEGY

Compared to linear system, nonlinear system has some high efficient characteristics in many areas. Given a simple example, considering system $\dot{x} = w(t) + u$, $w(t)$ is the disturbance, control signal $u(t)$ is designed to stabilize the whole system. For linear feedback control $u = -kx$, the steady error of system is $e = w(t)/k$ ($k > |w(t)|$). By choosing nonlinear feedback control $u = -k|x|^{\alpha} sign(x)$ ($0 < \alpha < 1$), the steady error of closed loop is reduced to $e = |w(t)/k|^{1/\alpha}$. That means proper nonlinear feedback control can restrict the effect of disturbance significantly. Based on nonlinear feedback, the nonlinear auto-disturbance rejection controller is composed of three parts (shown in Fig.1): tracking-differentiator (TD), extended state observer and nonlinear state error feedback control law (NLSEF) [8].

The key part of ADRC is (N+1)th order ESO, which uses nonlinear state feedback to realize the linearization of uncertain nonlinear systems. For an uncertain system

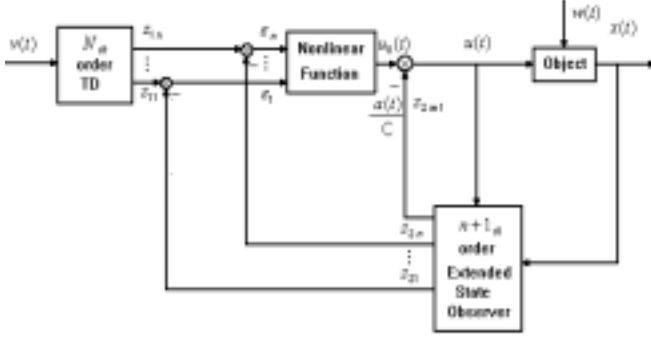$$x^{(n)} = f(x, \dot{x}, \cdots, x^{(n-1)}, t) + w(t) + u(t) \qquad (1)$$

Fig. 1. The Block Diagram of ADRC

where $f(t)$ represents uncertain function, $w(t)$ is an unknown disturbance, $u(t)$ is the control law and $x(t)$ is the measurable state variable. Its state space equation can be written as:

$$\begin{cases} \dot{x}_1 = x_2 \\ \qquad \vdots \\ \dot{x}_{n-1} = x_n \\ \dot{x}_n = f(x, \dot{x}, \cdots, x^{(n-1)}, t) + w(t) + cu \end{cases} \qquad (2)$$

Unlike full order (Nth order) state observer, ESO utilizes (N+1)th order (full order plus 1) state observation to achieve feedback linearization (shown as follows).

$$\begin{cases} \dot{z}_1 = z_2 - g_1(z_1 - x(t)) \\ \qquad \vdots \\ \qquad \vdots \\ \dot{z}_n = z_{n+1} - g_n(z_1 - x(t)) + cu \\ \dot{z}_{n+1} = -g_{n+1}(z_1 - x(t)) \end{cases} \qquad (3)$$

where

$$g_i(z) = \beta_{0i} fal(z_1 - x(t), \alpha_i, \delta) \qquad i = 1, \cdots, n+1$$

$$fal(\varepsilon, \alpha, \delta) = \begin{cases} |\varepsilon|^{\alpha} \, \mathrm{sgn}(\varepsilon), & |\varepsilon| > \delta \\ \varepsilon \big/ \delta^{1-\alpha}, & |\varepsilon| \le \delta \end{cases}$$

In ESO, lower order derivative is obtained by integrating the higher order derivatives. Differential operation is not needed anymore. Therefore, the differential signal is obtained without noises. Furthermore, the signal of (N+1)th state variable $z_{n+1}(t)$ reveals the information about disturbances and plant uncertainties in the control system. When the nonlinear functions $g_i(z)$ and their related parameters are properly selected, the state variables $z_i(t)$ $i = 1, \cdots, n$ of ESO will converge to the observed state variables $x(t)$ and its derivatives quickly. In addition, if the derivative of $f(x, \dot{x}, \cdots, x^{(n-1)}, t) + w(t)$ has some boundary, the overall effect of the external and internal disturbances imposed on the system can be observed by $z_{n+1}(t)$ successfully, even though $f(t)$ and $w(t)$ may be still unknown. Similar to input-output feedback linearization, ESO can be treated as some kind of dynamic feedback

lineariztion, but its architecture is not determined by the actual expression of system under control, but only affected by the range of its variation rate. Therefore, this observer has very good robustness and adaptability.

Tracking-Differentiator (Nth order TD in the Fig.1) is a dynamic system that it can arrange the transition process according to the input reference signal and the system under control. Its output is used as the given input signal of NLSEF. The mathematic function of TD is given below:

$$\begin{cases} \dot{z}_1 = z_2 \\ \dot{z}_2 = -rfal(z_1 - v, \alpha, \delta) \end{cases} \qquad (4)$$

where $v(t)$ is the input signal, $z_1(t)$ is the modulated estimation of $v(t)$ and $z_2(t)$ is the derivative of $v(t)$. From (4), we can see TD function is a nonlinear structure with linear intervals. It is obvious that this topology can fully utilize the nonlinear characteristics for large signals, and at the same time, the phenomenon of chatting is avoided near the original point. Furthermore, TD smoothes the sharp changes in the input signal, so that both the fast response and the reduced overshoot can be guaranteed.

Comparing the difference between the outputs of tracking-differentiator $z_{11}, \cdots, z_{1n}$ and those of extended state observer $z_{21}, \cdots, z_{2n}$, nonlinear state error feedback control law $u_0(t)$ is used to drive the state trajectory to the desired reference signal (shown in Fig.1).

$$u_0 = k_1 fal(\varepsilon_1, \alpha, \delta) + \cdots + k_n fal(\varepsilon_n, \alpha, \delta) \qquad (5)$$

where $\varepsilon_1 = z_{11} - z_{21}, \varepsilon_2 = z_{12} - z_{22}, \cdots, \varepsilon_n = z_{1n} - z_{2n}$

With the help of modeling uncertainty and disturbance estimation $z_{n+1}(t)$, online compensation is made by $u(t) = u_0(t) - z_{n+1}(t)$. The desired behaviors of the control system such as tracking, regulation and stability are achieved.

III. ADRC FOR INDUCTION MOTOR

Based on assumptions that stator windings are sinusoidally distributed, air gap is uniform and saturation are negligible, the state space model of a squirrel case induction motor in a synchronous d-q reference frame can be described by fourth order nonlinear differential equation:

$$\begin{cases} \dot{i}_{d1} = -k_1 i_{d1} + k_2 \psi_{d2} + i_{q1}\omega_1 + \dfrac{1}{\sigma} u_{d1} \\ \dot{\psi}_{d2} = \dfrac{L_m}{T_r} i_{d1} - \dfrac{1}{T_r}\psi_{d2} \\ \dot{\omega}_r = k_3\psi_{d2}i_{q1} - T_L n_p / J \\ \dot{i}_{q1} = -k_1 i_{q1} - \dfrac{L_m}{\sigma L_r}\psi_{d2}\omega_r - i_{d1}\omega_1 + \dfrac{1}{\sigma} u_{q1} \end{cases} \qquad (6)$$

where

$$T_r = \frac{L_r}{R_r} \qquad\qquad \sigma = L_s - \frac{L_m^2}{L_r}$$

$$k_1 = \frac{R_s L_r^2 + R_r L_m^2}{\sigma L_r^2} \qquad k_2 = \frac{R_r L_m}{\sigma L_r^2} \qquad k_3 = \frac{n_p^2 L_m}{J L_r}$$

u_{d1}, u_{q1}	d - axis(q - axis) stator voltage
i_{d1}, i_{q1}	d - axis(q - axis) stator current
ψ_{d2}, ψ_{q2}	d - axis(q - axis) rotor flux
ω_1	rotating speed of the coordinate
ω_r	rotor angular speed
T_L	load torque
R_s, R_r	stator and rotor resistances
L_s, L_r, L_m	stator, rotor and mutual inductances
J	rotor inertia
n_p	pole pairs

It is shown from the above equations that
(1) The system is nonlinear due to the coupling parts between state variables.
(2) The variation of motor parameters and load conditions will deteriorate the performance of the drive system.

Here, it is assumed that $\omega_r, \psi_{d2}, i_{d1}, i_{q1}$ and their derivatives exist and are continuous. As it is shown in (6), the rotor flux loop is mainly controlled by first and second item of (6); the speed loop is affected mainly by the third and fourth item of (6). However, these two loops have some intersect coupling parts, which could lead to sluggish dynamics both in speed and flux loop.

By differentiation, the 2nd derivative of flux is obtained as follows:

$$\ddot{\psi}_{d2} = -\frac{1}{T_r}\dot{\psi}_{d2} + \frac{L_m}{T_r}k_2\psi_{d2} + \frac{L_m}{T_r}(-k_1 i_{d1} + i_{q1}\omega_1) + \frac{L_m}{T_r\sigma}u_{d1} \quad (7)$$

Compared to (1), if the coupling part of (7)-- $\frac{L_m}{T_r}(-k_1 i_{d1} + i_{q1}\omega_1)$ is regarded as the modeling uncertainty or internal disturbance of system, then we can rewrite (7) as:

$$\ddot{\psi}_{d2} = -\frac{1}{T_r}\dot{\psi}_{d2} + \frac{L_m}{T_r}k_2\psi_{d2} + w_{11}(t) + \frac{L_m}{T_r\sigma}u_{d1} \quad (8)$$

Where $w_{11}(t) = \frac{L_m}{T_r}(-k_1 i_{d1} + i_{q1}\omega_1)$

Similarly, the coupling part in the differential functions of ω_r and i_{q1} can be treated as internal disturbance as following:

$$\begin{cases} \dot{\omega}_r = k_3\psi_{d2}i_{q1} + w_{21}(t) \\ \dot{i}_{q1} = -k_1 i_{q1} + w_{31}(t) + \frac{1}{\sigma}u_{q1} \end{cases} \quad (9)$$

Where

$$w_{21}(t) = -T_L n_p / J \quad w_{31}(t) = -\frac{L_m}{\sigma L_2}\psi_{d2}\omega_r - i_{d1}\omega_1$$

If we select the control voltage reference as:

$$u_{d0} = \frac{w_{11}(t)}{L_m/(T_r\sigma)} + u_{d1} \quad (10)$$
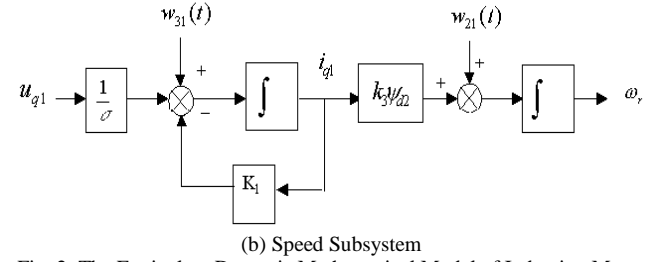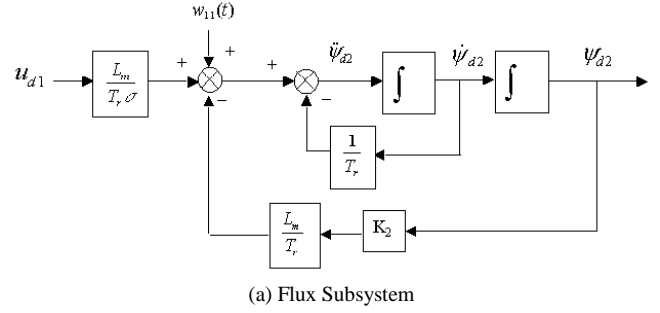

(a) Flux Subsystem

(b) Speed Subsystem

Fig. 2. The Equivalent Dynamic Mathematical Model of Induction Motor

$$I_{q0} = i_{q1} + w_{21}(t)/(k_3\psi_{d2}) \quad (11)$$

$$u_{q0} = w_{31}(t)\cdot\sigma + u_{q1} \quad (12)$$

then, the coupling part between the flux loop and speed loop can be completely eliminated. The dynamic functions of the whole system can be simplified as:

$$\ddot{\psi}_{d2} = -\frac{1}{T_r}\dot{\psi}_{d2} + \frac{L_m}{T_r}k_2\psi_{d2} + \frac{L_m}{T_r\sigma}u_{d0} \quad (13)$$

$$\dot{\omega}_r = k_3\psi_{d2}I_{q0}$$

$$i_{q1} = -k_1 i_{q1} + \frac{1}{\sigma}u_{q0}$$

Just as mentioned above, the dynamic model of induction motor is decoupled into two linear subsystems: flux subsystem and speed subsystem (shown in Fig.2). It is obvious from Fig. 2 that the precise decoupling of flux and speed control and exact linearization can be achieved if the ESO can realize the state and model disturbance estimation accurately. So, it is convenient to use a 2nd ADRC to give the flux control signal u_{d1}, and use two 1st ADRC in cascade to send out speed and current control signal I_{q0}, u_{q1} [9].

Considering the external disturbance and parameter variation, we use the rotor resistant variation and load disturbance as an example (for it happens most frequently in induction motor control), then (8), (9) can be rewritten as follows,

$$\ddot{\psi}_{d2} = -\frac{1}{T_r}\dot{\psi}_{d2} + \frac{L_m}{T_r}k_2\psi_{d2} + w_{11}(t) + \frac{L_m}{T_r\sigma}u_{d1} + w_{12}(t) \quad (14)$$

$$w_{12}(t) = (\frac{1}{T_r} - \frac{1}{T_r'})\dot{\psi}_{d2} + (\frac{L_m}{T_r'}k_2' - \frac{L_m}{T_r}k_2)\psi_{d2} + (\frac{L_m}{T_r'\sigma} - \frac{L_m}{T_r\sigma})u_{d1}$$

$$\begin{cases} \dot{\omega}_r = k_3\psi_{d2}i_{q1} + w_{21}(t) + w_{22}(t) \\ \dot{i}_{q1} = -k_1 i_{q1} + w_{31}(t) + \frac{1}{\sigma}u_{q1} + w_{32}(t) \end{cases} \quad (15)$$
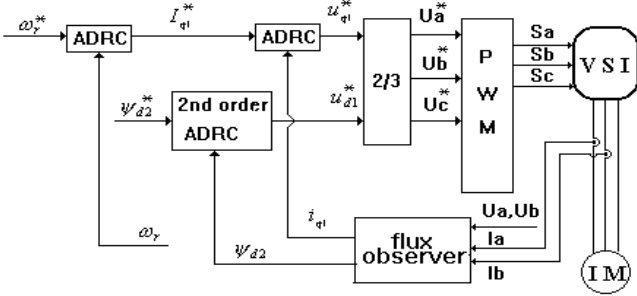
Fig. 3. The Control System of Induction Motor

where

$$w_{22}(t) = \Delta k_3 \psi_{d2} i_{q1} + \Delta T_L n_p / J$$

$$w_{32}(t) = \Delta k_1 i_{q1} + \Delta(\frac{1}{\sigma}) u_{q1}$$

In the above model, the external load change and internal parameter variation are all treated as disturbances imposed on the control system. Because the variation range of load and parameter change is finite, we can estimate and compensate overall influence of model parameter variation and external disturbance by properly selecting the functions and related parameters of ESO and NLSEF. And these functions and parameters of ADRC are all independent of object under control. From the above analysis, it is shown that the closed loop motor drive system under ADRC control does not depend on the accurate mathematical model of induction motors. Therefore, the robustness and adaptability of the control system is significantly improved.

Fig.3 shows the proposed ADRC for induction motor. In order to achieve the rotor angular speed and the rotor flux regulation, the controller includes two distinct control loops: the flux loop which employs one 2nd ADRC to regulate the rotor flux; the speed loop, which employs two 1st order ADRC in cascade to control the rotor speed ω_r and q-axis stator current i_{q1}.

IV. RESULTS

Computer simulation and experiments are conducted to evaluate the performance of proposed ADRC. The example tested in the paper is the prototype of a typical 3-phase 2.2 kW induction motor whose parameters are given as follows:

Rs=2.92 Ω	Rr=1.92 Ω	Ls=0.371 H
Lr=0.371 H	Lm=0.358 H	Polepairs=2
$J = 0.1 kg \cdot m^2$	Rated Speed$= 1430$ rpm	

A. Simulation Results

All simulations are done with a load torque change applied to the induction motor. To see the influence of the proposed controller, the performances of ADRC and classic PID controller are compared in the same condition. In addition, in order to constraint the noises that exist in the detected signals,

the coefficient of differentiator in PID controller is small.

Fig. 4 shows the actual and estimated rotor angular speed ω_r during acceleration. At t=1.1s, load torque $T_L = 15 N \cdot m$ is applied to the induction motor. Fig. 5 shows the derivative of rotor angular speed including the actual value and the value estimated by ESO. The simulation traces show that it is difficult to distinguish between the observed values and its reference signals. These indicate that the extended state observer can track the state variables of the induction motor and their derivatives successfully.

Fig. 6 shows dynamic responses of ADRC and PID controller with step disturbance load ($T_L = 15 N \cdot m$). For ADRC, the speed response under rated speed shows no overshoot and it settles down quickly to a steady state without steady state error. In addition, under the control of ADRC, the peak value of speed vibration (1.5 rpm) due to sharp change of load torque is smaller than that of classical PID controller (1.8 rpm).

In order to evaluate the dynamic performance of ADRC under wide operation range, the parameters of the ADRC and PID controller have been optimized at rated speed (1430 rpm). Then, the same controllers are applied to regulate the induction motor at low speed (10 rpm) without changing their parameters. It can be seen from Fig.7 that the performances of PID controller deteriorate, but ADRC can still maintain its excellent performance. It demonstrated ADRC could maintain its good dynamics and robustness to load disturbances in various operating conditions.

B. Experiment Results

Fig 8, 9 show the speed response curves of the induction motor with load torque $T_L = 6 N \cdot m$ while setting rotor speed is changed. The chatting in the speed response of PID controller (shown in Fig.9) is due to the fact that its tuning is parameter and condition dependent. It could not work well under different operation condition without modifying its parameters. From these figures, we can see that the ADRC can maintain better dynamic performance and adaptability than PID controller over wide speed range.

In order to verify the robustness of ADRC under parameter variation, we imitate the rotor resistor changes by resetting the value of given rotor resistance in the model of induction motor to be approximately 50% lower (from $1.92\Omega \rightarrow 1.0\Omega$) or 25% higher (from $1.92\Omega \rightarrow 2.5\Omega$) than that of the actual rotor resistance separately. After that, we operate ADRC and PID controller under the same working situation. From Fig. 10, we can see that the ADRC can maintain no overshoot and small transient time during start up while dynamic performance of PID controller has deteriorated. Fig.11 to Fig.14 show the experimental tests of ADRC and PID controller under given rotor resistance changes. We can see that the dynamic performance of PID controller deteriorates significantly, its transient time prolonged and some vibrations
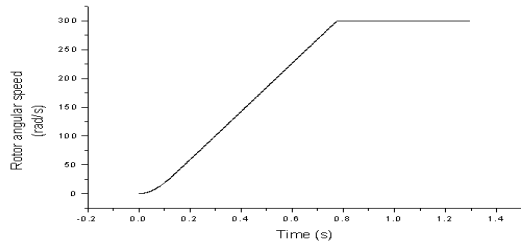
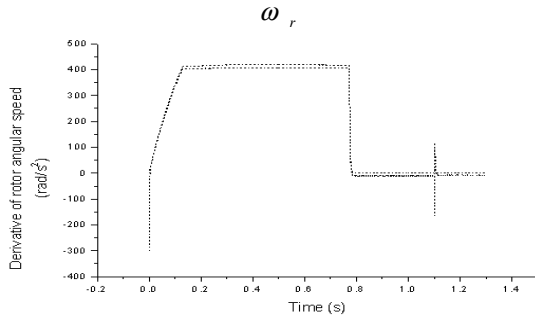Fig. 4 Actual (solid line) and estimated (dashed line) rotor angular speed ω_r

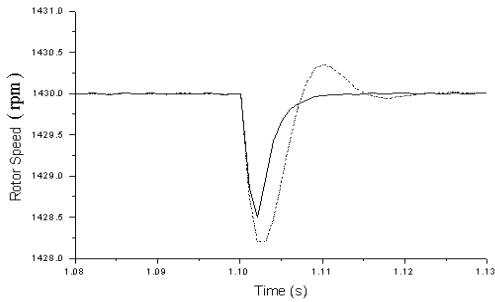Fig.5 Actual (solid line) and estimated (dashed line) rotor angular speed derivative

Fig. 6 Dynamic speed responses of ADRC (solid line) and PID controller (dashed line) due to load torque change (from $0-15\ N\cdot m$) at rated speed
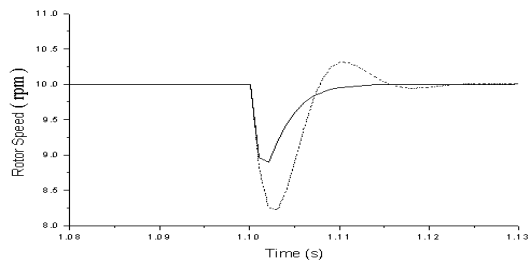

Fig. 7 Dynamic responses of speed regulation at low speed (10 rpm) --- Using ADRC (solid line); Using PID controller (dashed line)
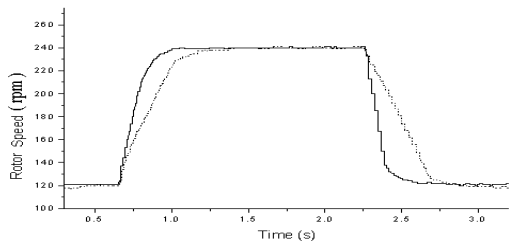

Fig. 8 Dynamic speed responses of induction motor (changed from 120 to 240rpm)--- ADRC (solid line); PID controller (dashed line)
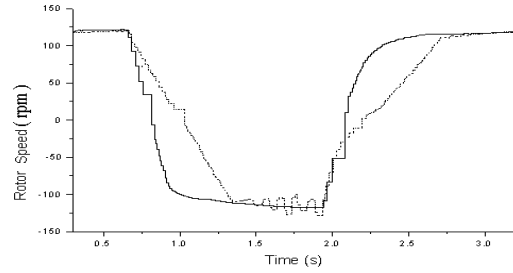
Fig. 9 Dynamic speed responses of induction motor (changed from 120 to –120rpm) --- ADRC (solid line); PID controller (dashed line)
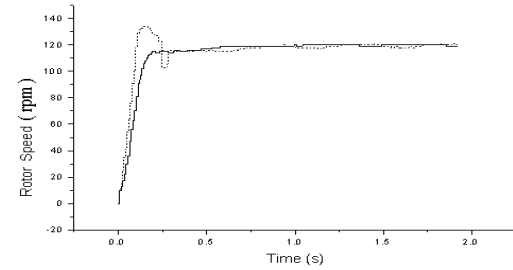
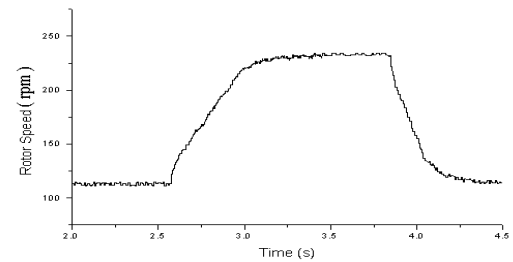Fig. 10 Dynamic speed responses of induction motor when starting up under rotor resistant change (from $1.92\Omega\rightarrow1.0\Omega$ --- ADRC (solid line); PID controller (dashed line)
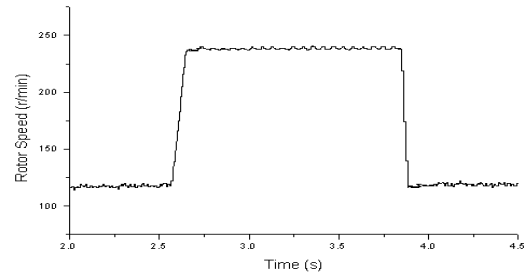
(a)   ADRC

(b) PID Controller

Fig. 11 Dynamic speed responses of induction from 120 to 240rpm under rotor resistant change (from $1.92\Omega\rightarrow1.0\Omega$)
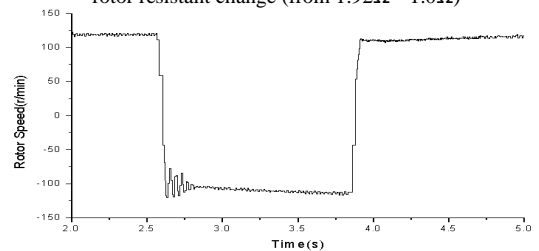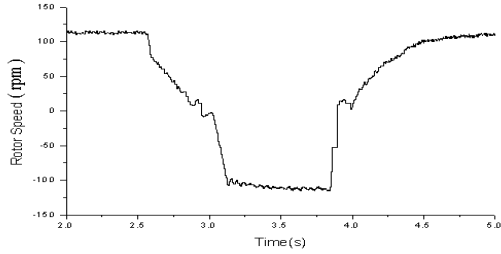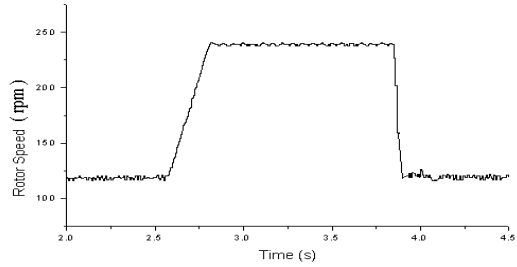

(a) ADRC

(b) PID Controller

Fig. 12 Dynamic speed responses of induction from 120 to –120rpm under rotor resistant change (from 1.92Ω→1.0Ω)
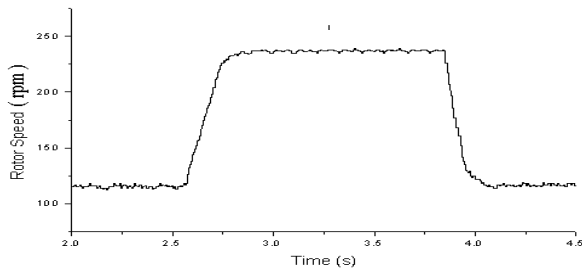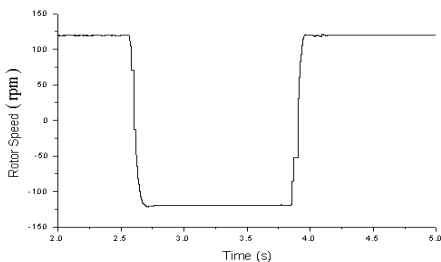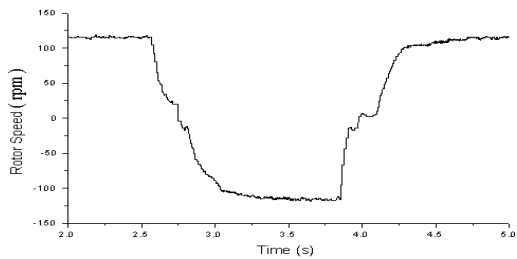

(a) ADRC

(b) PID Controller

Fig. 13 Dynamic speed responses of induction from 120 to 240rpm under rotor resistant change (from 1.92Ω→2.5Ω)

(a) ADRC

(b) PID Controller

Fig. 14 Dynamic speed responses of induction from 120 to –120rpm under rotor resistant change (from 1.92Ω→2.5Ω)

emerged during acceleration and deceleration. But ADRC can still maintain good speed regulation in spite of parameter changes. From these figures, it can be noted that ADRC can achieve good robustness and adaptability to external and internal disturbances.

V. CONCLUSION

In this paper, a new robust nonlinear controller for induction motors has been developed and demonstrated. The basis of Auto-Disturbance Rejection Controller is extended state observer and nonlinear feedback control. ADRC is used to implement the state estimation and compensation of motor parameter's change and load variation. The major advantage of the proposed method is that the closed loop characteristics of the motor drive system do not depend on the exact mathematical model of induction motor. Unlike PID controller, no derivative calculation is needed. Comparisons were done in details between ADRC and classical PID controller. It is concluded that the proposed control algorithm produces better results for dynamic operation than PID controller. As verified with simulation and experiment results, the proposed ADRC control system is robust against the modeling uncertainty and the external disturbance. These results open new perspectives on utilization of nonlinear topologies on vector control, and indicate that such scheme can be applicable to industry application where high dynamic performance is preferred.

REFERENCES

[1]   Special Issue on Power Electronics and Motion Control, *Proc. IEEE*, vol. 82, no. 8, Aug. 1994

[2]   R.S.Cabrera and J.Morales, "Some results about the control and observation of induction motors", in *Proceedings of the 1995 IEEE American Control Conference*, 95CH35736, pp. 1633-1637.

[3]   Y. Ping, D. Vrancic, and R. Hanus, "Anti-windup, bumpless, and conditioned transfer techniques for PID controllers," *IEEE Trans. Contr. Syst. Technol.*, vol. 16, pp. 48-57, July 1996.

[4]   K. J. Astrom and T. Hagglund, *Automatic Tunning of PID Controllers*, Instrument Society of America, Research Triangle Park, NC, pp.3-28, 1998.

[5]   N. J. Krikelis and S. K. Barkas, "Design of tracking systems subject to actuator saturation and integral wind-up", in *Int. J. Control*, vol. 39, no. 4, pp. 667-682, 1984.

[6]   Chen Jie,Li Yongdong, "Virtual Vectors Based Predictive Control of Torque and Flux of Induction Motor and Speed Sensorless Drives", *IEEE IAS 99*, pp 2606-2613.

[7]   C. Cecati, G. Guidi, "An adaptive non-linear control algorithm for induction motor", in *Proceedings of the 1996 IEEE IECON*, vol.1, pp.326-331.

[8]   J. Han, "Auto-disturbances-rejection Controller and It's Applications", *Trans. Control and Decision*, China, vol.13, no.1, pp19-23, 1998.

[9]   Guang Feng, Lipei Huang and Dongqi Zhu, "A Nonlinear Auto-Disturbance Rejection Controller for Induction Motor", *IEEE IECON'98*, vol.3, pp1509-1514.